



# A comparative study between a miniaturized liquid junction built in a capillary gap and semi-open capillaries for nL sample infusion to mass spectrometry

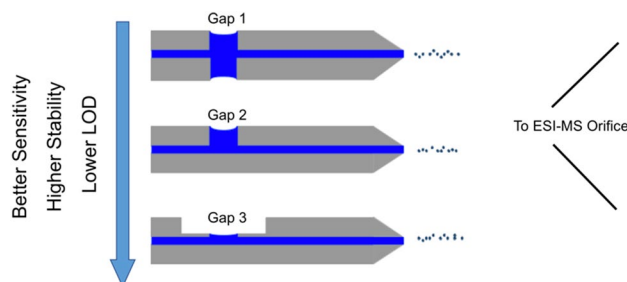
Sahar Ghiasikhou<sup>1</sup> · Adrien Marchand<sup>1</sup> · Renato Zenobi<sup>1</sup>

Received: 3 October 2018 / Accepted: 20 March 2019 / Published online: 30 March 2019  
© Springer-Verlag GmbH Germany, part of Springer Nature 2019

## Abstract

This study introduces a novel design for a microfluidic element used in a high-throughput screening mass spectrometer autosampler. The original design of the sampler consists of a liquid bridge formed in a micrometer gap between two capillaries. This liquid bridge is used to receive the sample, which is later ionized and analyzed by mass spectrometry. However, this liquid bridge is difficult to establish and maintain for long time periods, making the screening of large libraries of compounds a tedious task. The improvement described here consists in replacing the liquid bridge by a single pierced capillary, called “semi-open capillary”. The fabrication of semi-open capillaries is explained. To achieve an optimum structure, two different machining methods were tested, laser ablation and electro-discharge micromachining. The advantages of this design over the previous one include reduction of the dead volume and that of the sample dilution, as well as higher stability. Characterizations of the repeatability and the limit of detection (LOD) show that the optimized semi-open capillary leads to nearly twofold lower LOD when compared to the original liquid bridge.

## Graphical Abstract



**Keywords** High-throughput screening · Capillary gap sampler · Semi-open capillary · Laser ablation · Electro-discharging machining · Sensitivity

**Electronic supplementary material** The online version of this article (<https://doi.org/10.1007/s10404-019-2229-7>) contains supplementary material, which is available to authorized users.

✉ Renato Zenobi  
zenobi@org.chem.ethz.ch

<sup>1</sup> Department of Chemistry and Applied Biosciences, ETH Zurich, 8093 Zurich, Switzerland

## 1 Introduction

The path from studying and understanding a disease to introducing a potent treatment in the market is a long, complex, expensive, and high-risk process. Drug discovery and pre-clinical stages consume a lot of time (and money) during this process. It takes years of research to study huge libraries of chemical compounds. High-throughput screening (HTS) allows researchers to quickly conduct millions of chemical, genetic, or pharmacological tests within a short time; hence,

HTS is in great demand (Ma et al. 2005). Therefore, high-throughput screening is a key step in drug discovery, due to the immense savings in time and money which it offers (<https://www.statista.com/statistics/765535/drug-discovery-market-worldwide-by-segment-globally/>; Bleicher et al. 2003).

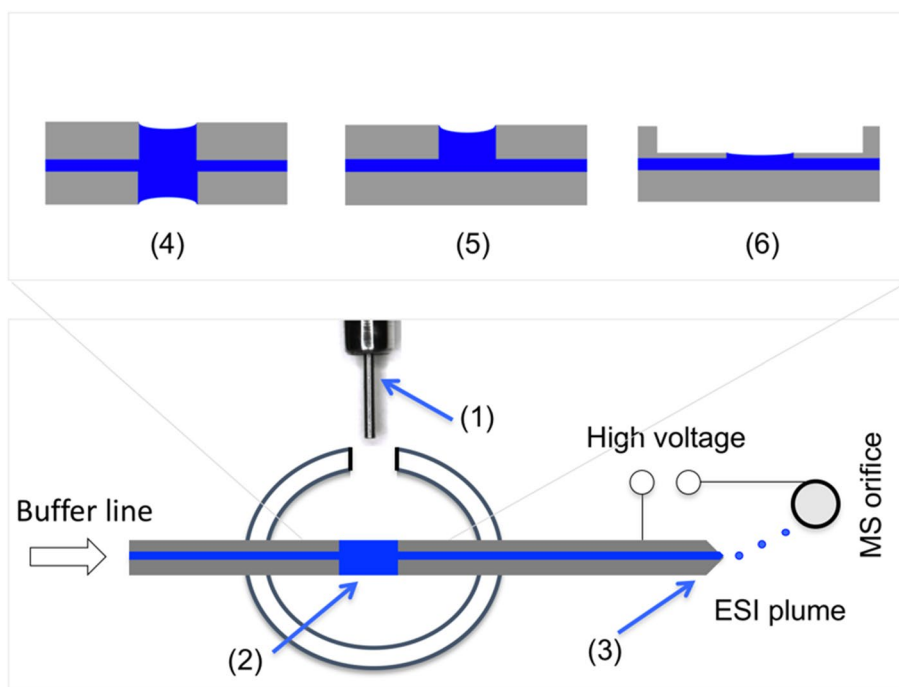
HTS coupled with Mass Spectrometry (MS) is a powerful tool to analyze a large number of compounds. During the last decades, the development of high-throughput samplers for MS got a lot of attention. Most of them are based on microfluidic technology (Sun and Kennedy 2014; Chen et al. 2005, 2012; Mao et al. 2013). First, microfluidics allows a better control of fluids and physical parameters. Second, using very a small amount of sample allows one to considerably decrease the screening cost. Finally, the possibility for automation and parallelization increases the throughput. Well-established microfluidic devices with a good level of maturity already provide rapid and high-throughput compounds analysis (van Reenen et al. 2014; Strohmeier et al. 2015; Ducrée et al. 2007; Gorkin et al. 2010; Keller et al. 2015). However, there remains room for improvement, for example, by decreasing even more the sample volume, increasing the speed and the robustness of the experiment, and developing multitasking approaches in terms of sample preparation.

When it comes to high-throughput drug screening of complex biological samples, an extra step of separation is often needed. Conventionally, MS is combined with gas or liquid chromatography (Sreekumar et al. 2009; Fiehn et al. 2000; Chen et al. 2009; Stark et al. 2011) or capillary electrophoresis (Wan et al. 2003; Chu et al. 1996) to extract the compounds of interest. However, such methods are often incompatible with HTS needs and can be expensive. In 2014, Jin et al. introduced the Swan-probe as an inexpensive tool for electrospray ionization (ESI)-MS HTS. It consists of a U-shaped capillary with a horizontal emitter tip. The probe is vertically grounded at the bottom of the U-shaped section, such that a hole of about 100  $\mu\text{m}$  forms as sample inlet. The sample is infused inside the capillary and later mixed and sprayed to ESI-MS by pumping the carrier solution through the capillary and placing the inlet on the droplet arrays on a multi-well plate. This probe can be dipped into an array of samples and, therefore, provides continuous sample screening. The sampling speed is of about 21 s per sample. The main drawback of this autosampler is the lack of precision in the fabrication method of the hole (Jin et al. 2014). In 2004, Ozbal et al. (2004) developed an ESI-APCI technique and hardware for HT discovery applications. In this method, an integrated microfluidic system is designed in a way that 1–5  $\mu\text{L}$  of sample gets delivered to a chromatography system for purification. The purified sample is then directed to a mass spectrometer for analysis. One injection cycle takes 5 s and the sample carryover issue is addressed using materials

such as Teflon, PEEK, and fused silica in the microfluidic circuits, as well as chemically modified surfaces. In addition, the entire system is flushed with aqueous and organic buffers between different samples, which, however, increases the analysis time. Screening of different inhibitors for acetylcholinesterase was performed as a proof of concept, and several potent inhibitors were identified. In 2012, Chen et al. (2012) developed an isotope labeling method performed in a microfluidic chip that is coupled to ESI-MS (SIL-chip-ESI-MS) for HT online analysis of cell metabolism. This platform combines a cell culture chamber and on-chip sample clean-up methods, including a micro-SPE column, connected via a microfluidic network. Such an integration followed by ESI-MS provides a multifunctional chip-based MS platform that has been used for qualitative and quantitative analyses of the metabolism of drug and cell interactions. In addition, there are several commercially available non-chip-based platforms that can be coupled to mass spectrometers. The best known ones are the Rapidfire from Agilent and the Nanomate from Advion (Jian et al. 2011; Zhang and Pelt 2004) In brief, using an automated sample uptake system, the Rapidfire reduces the injection cycle to 6–13 s per sample. A robot scans and moves the microwell plates automatically, so that a large number of samples can be analyzed without human supervision. In addition, it provides an automated online solid-phase extraction by injection of sample volumes  $> 10 \mu\text{L}$  into cartridges. On the other hand, the Nanomate enables the analysis of various samples without cross-contamination, using an automated pipette to deliver a few microliters to the mass spectrometer. Pneumatically assisted spraying through nano-electrospray nozzles can last up to several minutes. 400 independent nozzles are fabricated on one chip. Each nozzle is used only once to prevent any cross-contamination.

Finally, Roche has developed an autosampler, called Capillary Gap Sampler (Neu et al. 2013) (shown schematically in Fig. 1), a miniaturized sampling device that can be used as a platform for direct and fast uptake or extraction (Ghiasikhou et al. 2017) of a few nL of sample. A solid stainless-steel pin is used as sampling tool and the sample is desorbed in a micrometer-sized liquid bridge formed between two capillaries, one of them acting as an electrospray emitter. The bridge of 10–40 nanoliters of solution provides a continuous and clean medium for the sample to be introduced to the mass spectrometer. This design allows the system to be constantly ready for receiving new samples. The device allows fast (9–11 s), automated, and comprehensive analyses of various samples. The main application of the instrument is the direct online high-throughput readout of chemicals. The most highlighted advantages of such an autosampler over the conventional borosilicate emitters are that it allows high-number of low-volume samples to be introduced to MS orifice with high speed. In

**Fig. 1** Key parts of the Capillary Gap Sampler: sampling tool held by the robot arms (1), liquid bridge (2), ESI spray tip (3), capillary gap named “Gap 1” (4), semi-open capillary (fabricated by laser ablation) called “Gap 2” (5), and semi-open capillary (fabricated by EDM) introduced as “Gap 3” (6) sample receptors



addition, microfluidic capillaries are reusable for hundreds of injections, whereas, in the conventional version, each borosilicate emitter can only be used once. Exchanging the emitters for each sample is time consuming and costly, and can introduce errors. The second important advantage of such a concept for sample delivery is its ability to perform online reaction and solid-phase microextraction. Despite of all these advantages of the sampler over the borosilicate emitters, the current system is not easy to operate. The main reason is that the formation and stability of the liquid bridge depends on different factors such as the surface tension of the solution, the spray capillary voltage, the solution flow rate, the distance between the capillaries, the overpressure inside the chamber, and the surface composition of the capillaries and their geometries (Neu et al. 2016). The optimization of these parameters to keep the liquid bridge stable can be tedious, especially in the case of using high surface tension liquids.

In this paper, we present a comparative study between different configurations of the sample receptor in the Capillary Gap Sampler. We present a new design, where instead of injecting the sample into a liquid bridge between two different capillaries, it is injected into a semi-open capillary. The stability of the device is enhanced, which increases the robustness of the method. In addition, by optimizing the gap shape, we could minimize the dead volume of the system, which allows the sample to be less diluted, which, therefore, increases the limit of detection (LOD). The advantages of the new liquid connector shapes and the production of a semi-open capillary are discussed in the following sections.

## 2 Experimental section

### 2.1 Chemicals and Materials

Acetonitrile  $\geq 99.9\%$  (LC-MS CHROMASOLV), water (LC-MS grade), acetazolamide, and leucine enkephalin were purchased from Sigma-Aldrich (St Louis, MO, USA). In addition, diazepam, diazepam-d5, and nordiazepam were obtained from Sigma-Aldrich (The Woodlands, TX, USA) and stored at 4 °C. Methanol (LC-MS grade) was purchased from Fisher scientific (Loughborough, U.K). Formic acid (98–100%) and rhodamine B were purchased from Merck (Darmstadt, Germany). The stainless-steel capillaries for three different configurations have 320  $\mu\text{m}$  O.D. and 50  $\mu\text{m}$  I.D. (New Objective, Woburn MA, USA) with the same opening at the end, only different lengths for Gap 1 (50 mm) and Gap 2 and 3 (150 mm).

### 2.2 Equipment for detection (Mass Spectrometer), software, and buffer delivery

A synapt G2-S high definition (Waters, Manchester) mass spectrometer operated in positive mode was used for the experiments. The source temperature was set to 30 °C and the capillary voltage was set to 3.2 kV. The Masslynx 4.1 software was used for acquiring data. Buffer delivery was performed via a syringe pump (neMesys, Cetoni, Korbuss, Germany).

## 2.3 Sampler design

The heart of the setup is shown in Fig. 1. The sampler itself is compact and light (4.5 kg), and comprises a robot with three arms, a sampling tool, a sample storage plate, optics and a stand to be screwed to the mass spectrometer. The sampling tool is held and moved by the arms of a light microrobot (model PocketDelta, Asyril, Villaz-St-Pierre). The fast, pulsation free operation of the robot has a movement precision of 3  $\mu\text{m}$ . The sampling tool moves with a constant speed into the different wells of the microwell plate to perform the different steps of the pre-defined sampling process. Finally, the pin held by the robot is pushed into a pressurized chamber to deliver the sample to the liquid bridge. The pressurized chamber ( $V=0.65$  ml) is made of PEEK and held under a controlled overpressure. A ceramic injection port with a bore (which rotates by 90° between the open and close positions) acts as a valve for pressure sealing. Two capillaries inside the pressure chamber are positioned with a small gap of 300  $\mu\text{m}$  to form the liquid bridge. The first capillary is made of fused silica (360  $\mu\text{m}$  O.D.; 50  $\mu\text{m}$  I.D., Polymicro, Phoenix AZ, USA) and connected to a syringe pump. The solution is pumped through the capillaries at a controllable flow (discussed in the text). The second capillary with a tapered tip is made of stainless steel (320  $\mu\text{m}$  O.D.; 50  $\mu\text{m}$  I.D.; 50 mm length; New Objective, Woburn MA, USA). By applying a high voltage between the MS orifice and the stainless-steel capillary, the solution is sprayed. To monitor the shape of the liquid bridge, a CCD camera (model  $\mu$ -eye, VS Technology Cooperation, Tokyo, Japan) is placed in front of the chamber (Fig. 1). A feedback loop by adjusting the pressure in the chamber and the flow rate of the solution allows to maintain a stable bridge. Telecentric optics (VS Technology Cooperation) are also used for optical process control. More information and details can be found in a previous publication by Neu et al. (2013).

## 2.4 Preparation of semi-open capillaries

Two different micromachining methods, laser ablation and electro-discharge machining, were used to drill a hole into the stainless-steel capillaries. The process and optimization will be discussed in detail in the Results and discussion section.

# 3 Results and discussion

## 3.1 Design of the semi-open capillary

Long stainless-steel single capillaries (total length of 15 cm) were pierced using two different machining methods: laser ablation and electro-discharge machining (EDM).

First, to produce a semi-open capillary with an opening angle of approximately 90°, hereafter called Gap 2, we used laser ablation. In laser ablation, by irradiating the surface with a laser beam, material evaporates. The amount of material removed by the laser depends on the laser wavelength, the pulse length and duration, as well as the material's optical properties. This method was chosen, since the laser pulse can be precisely controlled over a wide range of time (from milliseconds to femtoseconds) (Laser ablation 2018). Laser ablation was performed at CSEM (Neuchâtel, Switzerland) using a TRUMICRO 5350 instrument with a 343 nm laser wavelength and 10 W mean power. The result of this fabrication method is shown in the following SEM images (Fig. 2a). They show redeposited material from the laser ablation. The tilted image displays the open channel. The other method used to make a hole was EDM, whereby a desired shape is obtained by rapid sparks on a surface. The sinker EDM process uses an electrically charged electrode that is configured to a specific shape to burn the geometry of the electrode into a metal component ([http://www.edmmachining.com/sinker\\_edm.htm](http://www.edmmachining.com/sinker_edm.htm)). EDM is a useful method to achieve such a configuration without residues left on the surface. For optimization of the hole geometry, we used the results from Neu et al. (2016) who described the influence of the capillary dimensions on the sample flush-out profile at the liquid bridge and along the spray capillary. They concluded that a reduction in the capillary wall thickness causes a significant decrease in peak width. The reason is the large dead zones in the liquid junction between two thick-walled capillaries. Clearly, smaller capillary inner diameter allows less sample dilution due to a smaller dead volume in the liquid connector. Therefore, the optimum configuration should provide the smallest dead zone possible. Accordingly, the structure of the hole was optimized. Using wire EDM, a part of the surface is then removed to reduce the thickness of the wall, and by sinker EDM, a hole was then machined in the center. The SEM image of such a structure is presented in Fig. 2b and called hereafter Gap 3.

Initially, a 115  $\mu\text{m}$  section of the capillary was removed by wire EDM followed by sinker EDM for making a hole ( $r=115$   $\mu\text{m}$ ) into it. Although surface roughness of the openings did not have any influence on the performance of the system, the fabrication quality improved a lot using EDM method compared to laser ablation.

To prevent spilling of the liquid, the outer surface of the stainless-steel capillaries was coated with a hydrophobic protein repelling agent [perfluoro-alkyl-nitro dopamine (PFAND)] (Rodenstein et al. 2010). Success of the coating procedure was evaluated by comparing X-ray photoelectron spectra before and after coating (Figure 1S supplementary information). In case of major fluctuations in pressure or flow rate, the liquid junction can be controlled by altering the flow rate or over pressure inside the chamber.



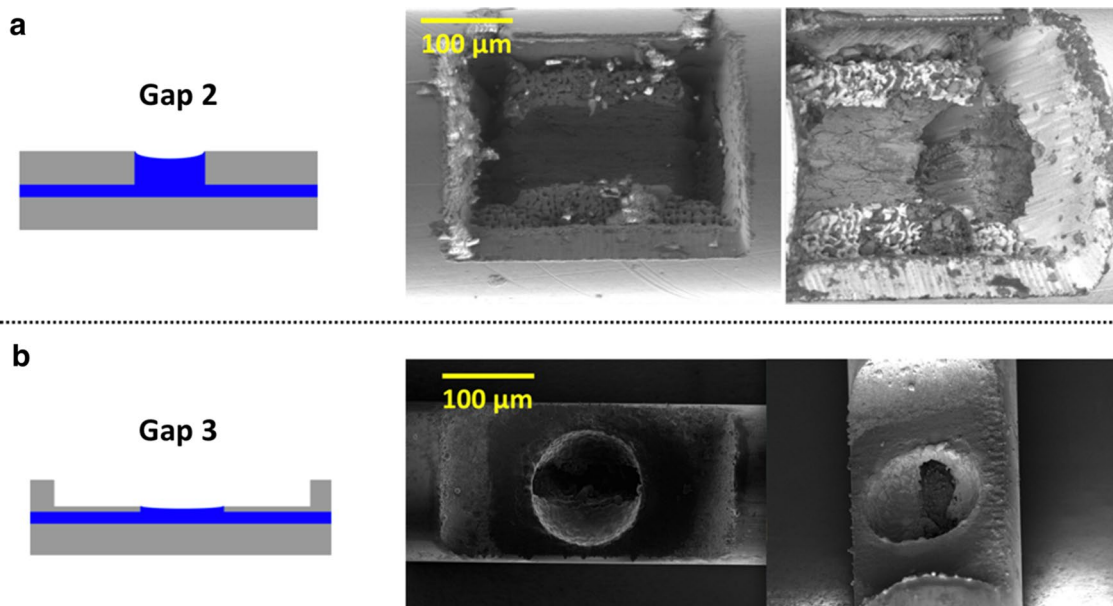


**Fig. 2** SEM images of the different holes in the stainless-steel capillary made by **a** laser ablation (300 μm \* 200 μm) (Gap 2) and **b** a combination of wire and sinker EDM method (Gap 3). 115 μm of the thickness is removed by wire EDM and a hole ( $r=115 \mu\text{m}$ ) is made inside

In the forthcoming sections, we will describe the advantages of the semi-open capillary over the classical double capillary configuration.

### 3.2 Increased liquid junction robustness with the semi-open capillaries

To characterize the robustness of the gap sampler, we sprayed different solutions with different surface tensions using the different capillaries. For each capillary, various combinations of flow rates and pressures were applied. Two different buffer compositions were tested: a relatively high (water: methanol 1:1, surface tension of 48 J/m<sup>2</sup>) and a low (pure acetonitrile, surface tension of 22 J/m<sup>2</sup>) (Wohlfarth 2008) surface tension liquid. Experiments were performed under different chamber pressures (0, 12, 25, 100 mbar). The flow rate of the buffer inside the capillary was set to 1 μL/min and increased by 1 μL/min every 100 s. Usually 100 s is long enough to collect an acceptable spectrum, and empirically, if a spray can stay stable for 100 s, then it can be considered stable for a long time.

The stability of the system can be directly assessed by the stability of the spray. Therefore, this evaluation was done based on the total ion current (TIC) chromatogram as a function of time. Experiments were stopped when flooding of the liquid out of the hole was observed by the real-time monitoring. The times reported in Fig. 3 correspond to the times during which the spray was stable (Fig. 2S and 3S in supplementary information present experimental results).

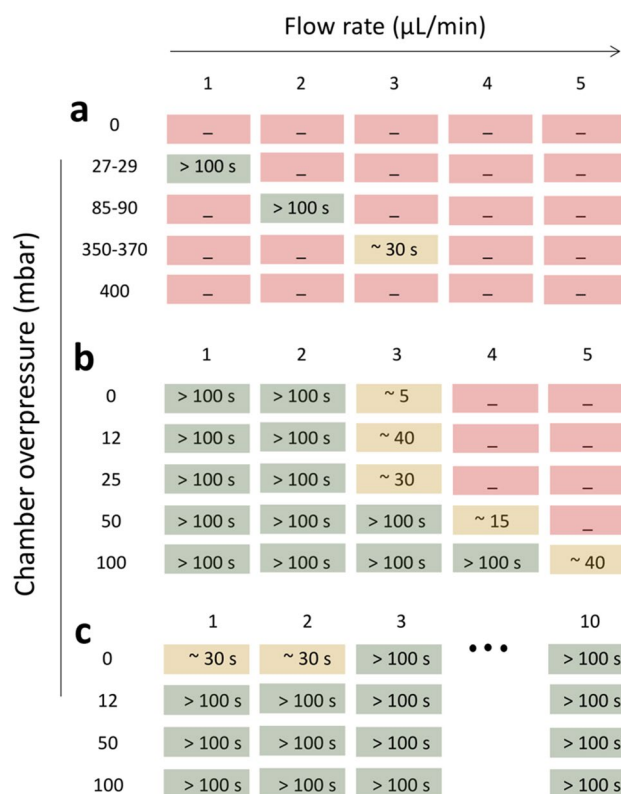


**Fig. 3** Pressure dependence experiment for Gap 1 and Gap 3, **a** Gap 1 (low surface tension solution). **b** Gap 3 (high surface tension solution). **c** Gap 3 (low surface tension solution). Different colors correspond to the liquid connector stability (green = stable, yellow = short-term stability, and red = not possible to make liquid connector) (color figure online)

Using the original system with an optimized gap distance (300  $\mu\text{m}$ ), the liquid bridge is mostly stable between 27 and 29 mbar for low surface tension solutions. Using the semi-open capillary, the pressure and flow rate range at which the signal is stable and the liquid connector is not flooding are significantly increased. Indeed, for low surface tension solutions, almost any combination of pressure (0–100 mbar) and flow rate (< 10  $\mu\text{L}/\text{min}$ ) tested were giving stable signals (Figure 3).

In addition, for high surface tension solutions, where it was almost impossible to get a stable spray with the previous design, the Gap 3 gives very good results. For example, depending on the flow rate, overpressures from almost 0 to 100 mbar can be used with flow rates of 1–4  $\mu\text{L}/\text{min}$ . In general, the results show that the system is compatible with a significantly wider range of flow rates at high chamber pressures. This can be explained by the fact that the back pressure caused by the high flow rate can be compensated by a high chamber pressure.

At flow rates lower than 1  $\mu\text{L}/\text{min}$ , broad peaks were observed, and with flows higher than 4  $\mu\text{L}/\text{min}$ , the back pressure needed exceeded the system tolerance back pressure compensation (max 400 mbar).

We believe the higher stability of Gap 3 compared to Gap 1 to be due to the fact that, in Gap 1, the liquid junction is entirely made up by liquid (called a “liquid bridge”). For Gap 1, if we assume formation of a liquid cylinder with a diameter of 320  $\mu\text{m}$  (= capillary diameter) and a length of 300  $\mu\text{m}$  (= gap distance), then roughly an area of  $6.03 \times 10^{-7} \text{ m}^2$  is exposed to atmosphere, which is, therefore, very sensitive to small fluctuations in pressure and flow rate. More effort and control are required to build and maintain such a liquid bridge, whereas the liquid in Gap 3 is flowing over a metal surface, which supports the uniformity of the liquid surface against variations in flow rate, pressure or voltage. The open surface area of the liquid in Gap 3 is  $4.15 \times 10^{-8} \text{ m}^2$ , i.e., 14.5 times smaller than that the exposed area for Gap 1.

### 3.3 Repeatability of sample infusion using semi-open capillaries

To illustrate the robustness of the new injection system using Gap 3, we performed 27 injections of rhodamine B [1.5  $\mu\text{M}$ , in acetonitrile/water 80:20 (v:v) + 0.1% formic acid], as shown in Fig. 4. The extracted ion chromatogram (XIC) of rhodamine B is recorded at  $m/z$   $443.4 \pm 0.3$ . The experimental conditions a, b, and c are described in Fig. 4. The capillary voltage, the flow rate, and the chamber pressure were varied for each part of the experiment.

The repeatability was evaluated from the relative standard deviation (RSD) of the peak intensities. For 27 injections at different experimental conditions using Gap 3, the RSD

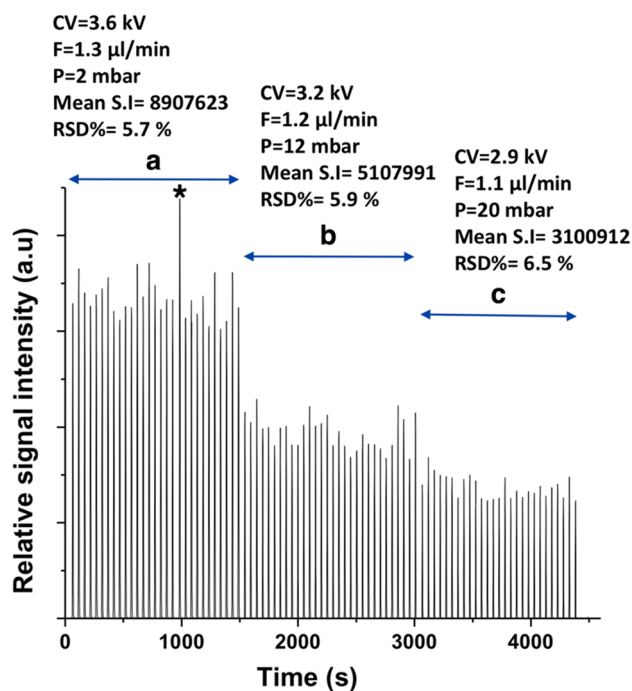


**Fig. 4** Representative injection sequence of Rhodamine B [1.5  $\mu\text{M}$ ], used for determining the repeatability of injections in different experimental conditions (*CV* capillary voltage, *F* flow rate, *P* chamber overpressure, *S.I.* signal intensity, *RSD* relative standard deviation). \*A data point was excluded in the RSD and mean value calculations in part due to instrumental error. Considering that point RSD and the average are 9.9% and 9,055,738, respectively

was less than 7%. This is an acceptable RSD and illustrates the repeatability of the experiments performed with Gap 3. The variations in the relative signal intensities in Fig. 4 are mainly coming from variations in the sample volume taken up by the sampling tool. This variation in volume uptake cannot be easily reduced. However, its effect on the signal intensity can be corrected using an internal standard directly mixed with the sample.

### 3.4 Less sample dilution and dead volume

To figure out the influence of the gap shape on the sample flush-out, we injected a mixture of cortisone, leucine enkephalin, and rhodamine B (1.5  $\mu\text{M}$  each) inside the liquid bridges formed between two capillaries and in the liquid connectors formed in the semi-open capillaries. To ensure that the liquid connector volume difference in three different gap shapes is only due to the different gap shapes, we kept the gap length (distance between two capillaries) the same as the lengths of the holes ( $\sim 300 \mu\text{m}$ ). All other experimental parameters including flow rate and capillary voltage were kept constant for both experiments.

Figure 5 shows representative elution peaks for cortisone for the three tested configurations. In Fig. 5a, the

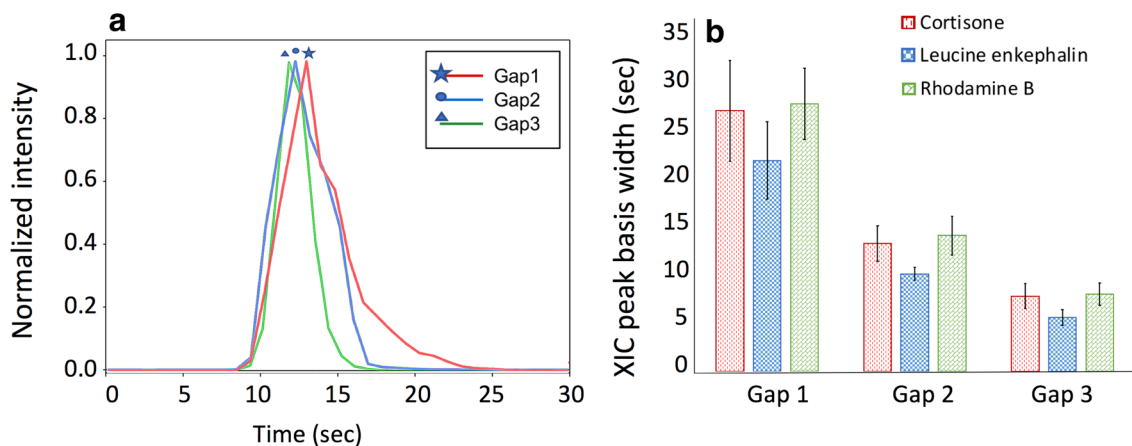


Fig. 5 Comparison of different sample peak widths for three configurations

normalized intensities of the extracted ion current are shown. These represent the normalized signal intensity of the ions reaching the detector as a function of time. The total ion current (TIC) sums the intensity of the entire mass range being detected at every point in the analysis, whereas an extracted ion current (EIC or XIC) shows the intensity of a certain *m/z* value versus time. An interesting result is that, with the semi-open capillaries, the peak widths are smaller compared to the dual capillary setup. In addition, there is a significant tailing with the latter that can be avoided using semi-open capillaries.

A mixture of three different compounds was injected 20 times and the results are shown in Fig. 5b. The average peak width for cortisone for the dual capillary system (Gap 1) and the semi-open capillary (Gap 3) is 27.7 and 7.7 s, respectively. Gap 2 gives intermediate peak widths. A similar effect is observed for leucine enkephalin and rhodamine B. In conclusion, using Gap 3, the peak width decreases by about 70% in comparison to Gap 1.

To explain why the peak elution widths are affected by the gap shape, we performed 3D COMSOL Multiphysics simulations for the different configuration (Fig. 6). These show the elution of an analyte from the gap to the outlet of the capillary. The legend is from dark red to blue, with dark red for the highest and blue for the lowest sample concentration, and is identical for all three gaps. At *t*=0, the sample is uniformly dispersed in the liquid junction. For all designs, the liquid flows from left to right with a 1  $\mu\text{L}/\text{min}$  flowrate. The flow is assumed to be laminar.

Different junction volumes and shapes yield to various dead zone sizes. This affects the distance along which the sample has to diffuse to reach the main stream. Compared to the gap sampler with two capillaries, both monolithic designs have much smaller dead volumes. A rough calculation shows the volume for Gap 3 hole to be about 1.5 nL, which is much less than the volume in the liquid bridge of the original capillary gap sampler (25 nL). More importantly, after removing a 115  $\mu\text{m}$  of the capillary wall,

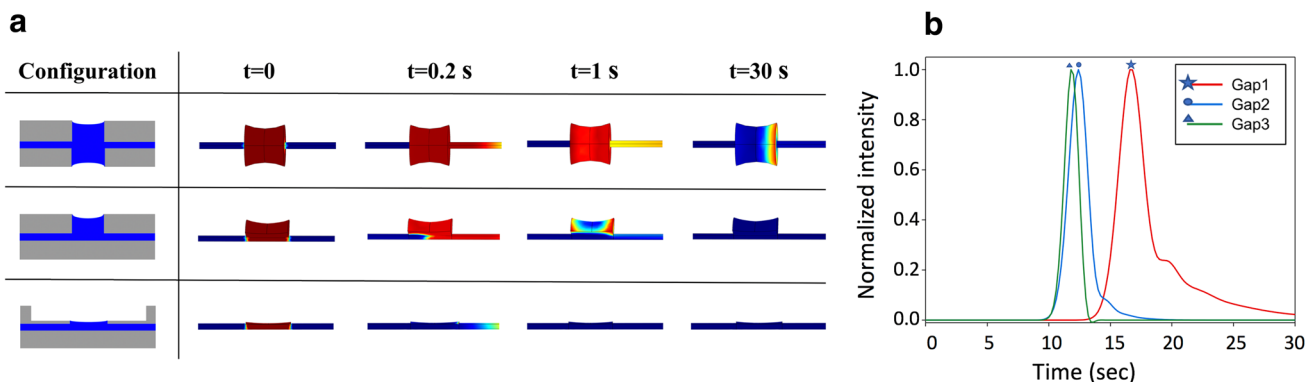


Fig. 6 a Flow COMSOL simulation for Gap 1, 2, and 3 at different times. Color code is from dark red to blue, with dark red for the highest and blue for the lowest sample concentration, and is identical for

all three gaps. b Normalized extracted ion current for small molecules (color figure online)

and considering the capillary's outer and inner diameter of 320 and 50  $\mu\text{m}$ , respectively, the diffusion distance for the analyte to reach the main flow is only 20  $\mu\text{m}$ . Already at  $t=0.2$  s, the difference in performances is clear: Gap 3 is almost empty, whereas Gap 1 still contains the majority of the sample. Gap 2 is similar to Gap 1, but its volume is only 25% of that of Gap 1. Thick capillary walls cause large dead zones. Using Gap 1, it takes more time for the analyte to reach and diffuse into the main stream of the flow. Some molecules are trapped inside the dead zone in the liquid bridge and remain there for more than 30 s.

Figure 6b shows the simulated normalized extracted ion current of a small molecule representing (cortisone, leucine enkephalin, or rhodamine B) for different gap configurations. The EIC was simulated by considering small molecule diffusion coefficients and a flow rate of 1  $\mu\text{L}/\text{min}$ . The results from Fig. 6a explain the tailing of the peaks for Gap 1 in Fig. 6b. Gap dimensions are explained in Fig. 2. The elution peak width results from the simulations are in good agreement with those obtained from the experiments. Replacing two capillaries with a single capillary, thus, benefits from less dead volume and, therefore, less memory effects.

### 3.5 System sensitivity

For the same amount of sample delivered to the gap, the signal is more intense for the semi-open capillaries.

Linearity and sensitivity of the system were investigated using diazepam, rhodamine B, and acetazolamide. Diazepam d5 was used as internal standard. Nordiazepam was used in the buffer line to account for changes in ionization efficiency. The compounds were chosen based on current applications of the sampler. For instance, acetazolamide and diazepam are two compounds of interest for performing solid-phase microextraction using the sampler. A dilution series of the mixture was injected into Gap 1 and Gap 3, four times each. Figure 7 shows the corrected mean signal intensities versus sample concentration for each analyte for the two capillary configurations.

Replacing Gap 1 (Fig. 7b) with Gap 3 (Fig. 7a), the LOD values for diazepam, rhodamine B, and acetazolamide changed from 50, 28, and 87 nM to 27, 12, and 50 nM respectively, which corresponds to nearly a factor of 2. LOD values were calculated based on the signal-to-noise ratio of 3:1 in extracted ion chromatograms for each analyte. As Fig. 7 presents, a nice linearity was achieved for all of the compounds using Gap 3. By performing more tests for low concentrations, the sensitivity was improved by 40–60% for the three compounds. By comparing the results, one can conclude that the semi-open capillary provides a better sensitivity for the system due to less sample dilution at the injection spot, which is very important for low concentration sample screening.

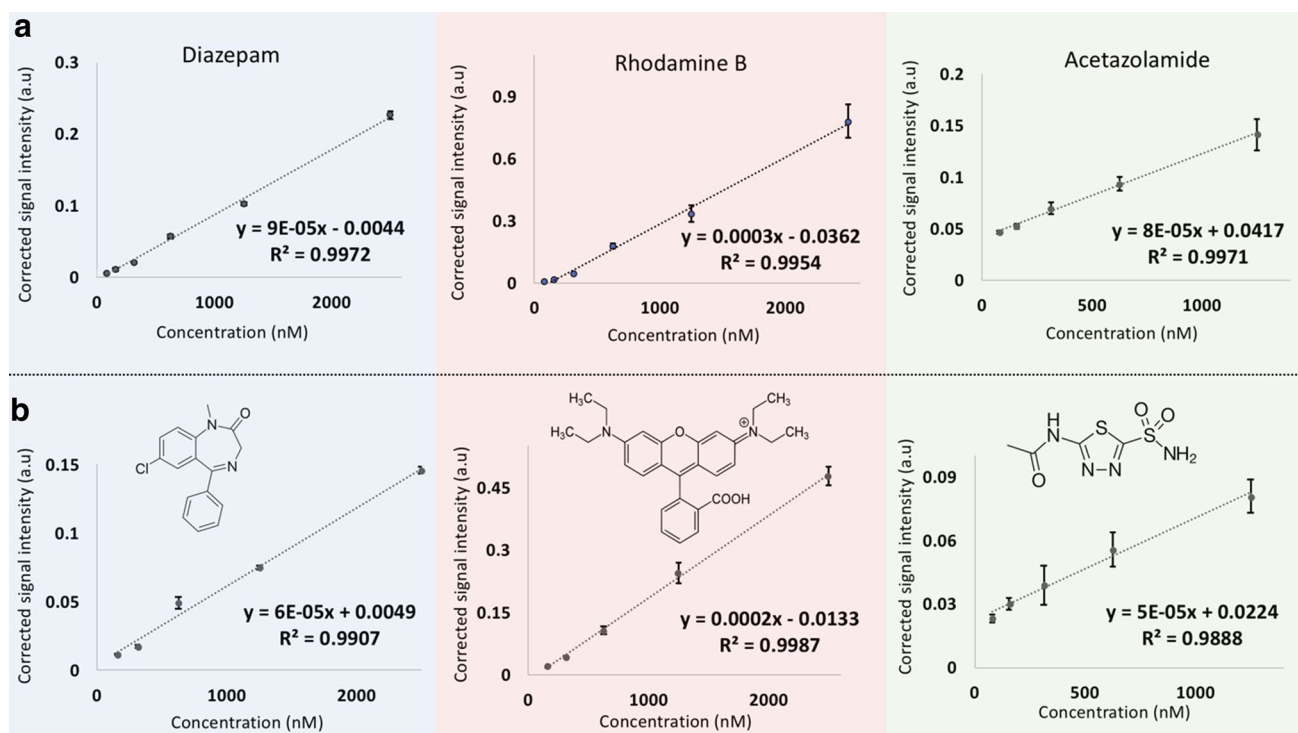


**Fig. 7** Corrected signal intensity (a.u) versus concentration (nM) of diazepam, rhodamine B, and acetazolamide using **a** Gap 3 and **b** Gap 1



## 4 Conclusions and outlook

In this paper, a new sample receptor design based on semi-open capillaries was introduced for the gap sampler technology. This design brings several advantages over the original configuration. Gap 3 shows a higher stability, and it is easier to build and maintain the liquid junction as compared to Gap 1. It also exhibits higher stability: the system is less dependent on the chamber overpressure and flow rate fluctuations. Not only the sampler is more robust to operate with Gap 3, but also quicker and almost user independent. The repeatability of the sample introduction under different conditions was tested and calculated. The calculated RSDs illustrate the higher reproducibility of the sampling process. Less sample dilution prior to ESI-MS results in higher sensitivity, which is crucial for analyzing low concentrations. The peak widths of individual analytes are compared for different configurations. A reduction of about 70% in peak width and about 50% in LOD prove the advantages of the new design. Using the new design, less peak tailing is observed as predicted by COMSOL flow simulations. After 0.2 s, there is almost no sample remaining in the liquid junction, whereas, in the conventional design, the sample is trapped close to the capillary walls and edges even 30 s after the injection. Improving this sampler to be more useable and stable for high surface tension solutions opens the doors toward many new applications. Screening non-covalent interactions which is mostly performed in aqueous solution can be done using the semi-open capillary. Being able to change the flow rate over a boarder range provides variety of sample residence times and makes it feasible to perform kinetic studies. Reagent mixing time inside the capillary can be easier to control by defining the hole position as well as altering the flow rate. Compared with the original capillary gap sampler, much less time is needed for the capillary alignment, and almost no time for building the liquid connection. On that account, this system is also quicker to operate.

**Acknowledgements** We gratefully thank Dr. Christof Fattinger (Roche) for his support in sampler development and Professor Ying Zhu (Department Chemistry, Zhejiang University) for helping in optimizing the structure of the hole. Moreover, we thank the Scientific Center for Optical and Electron Microscopy (ScopeM), a central technology platform of ETH Zurich, for providing us with resources and services in electron microscopy, the ETH Physics workshop for performing EDM for semi-open capillary preparation, and the SuSoS company in Dübendorf for providing us with a PFAND solution and for recording XPS data. Finally, we thank the Swiss National Science Foundation (SNSF) for funding this project (Grant Nos. 200020-159929 & 200020-178765).

## References

- Bleicher KH, Böhm H-J, Müller K, Alanine AI (2003) Hit and lead generation: beyond high-throughput screening. *Nat Rev Drug Discov* 2:369–378
- Chen H, Talaty NN, Takáts Z, Cooks RG (2005) Desorption electrospray ionization mass spectrometry for high-throughput analysis of pharmaceutical samples in the ambient environment. *Anal Chem* 77:6915–6927
- Chen YG, Kowtoniuk WE, Agarwal I, Shen Y, Liu DR (2009) LC/MS analysis of cellular RNA reveals NAD-linked RNA. *Nat Chem Biol* 5:879–881
- Chen Q, Wu J, Zhang Y, Lin J-M (2012) Qualitative and quantitative analysis of tumor cell metabolism via stable isotope labeling assisted microfluidic chip electrospray ionization mass spectrometry. *Anal Chem* 84:1695–1701
- Chu Y-H, Dunayevskiy YM, Kirby DP, Vouros P, Karger BL (1996) Affinity capillary electrophoresis—mass spectrometry for screening combinatorial libraries. *J Am Chem Soc* 118:7827–7835
- Drug discovery market worldwide by segment 2025 forecast|Statistic. Statista. <https://www.statista.com/statistics/765535/drug-discovery-market-worldwide-by-segment-globally/>. Accessed 21 June 2018
- Ducrée J et al (2007) The centrifugal microfluidic Bio-Disk platform. *J Micromech Microeng* 17:S103
- Fiehn O et al (2000) Metabolite profiling for plant functional genomics. *Nat Biotechnol* 18:1157–1161
- Ghiasikhou S, Fabricio da Silva M, Zhu Y, Zenobi R (2017) The capillary gap sampler, a new microfluidic platform for direct coupling of automated solid-phase microextraction with ESI-MS. *Anal Bioanal Chem* 409:6873–6883
- Gorkin R et al (2010) Centrifugal microfluidics for biomedical applications. *Lab Chip* 10:1758–1773
- How Sinker EDM Machining Works. [http://www.edmmachining.com/sinker\\_edm.htm](http://www.edmmachining.com/sinker_edm.htm). Accessed: 28 June 2018
- Jian W et al (2011) Evaluation of a high-throughput online solid phase extraction-tandem mass spectrometry system for in vivo bioanalytical studies. *Anal Chem* 83:8259–8266
- Jin D-Q, Zhu Y, Fang Q (2014) Swan probe: a nanoliter-scale and high-throughput sampling interface for coupling electrospray ionization mass spectrometry with microfluidic droplet array and multiwell plate. *Anal Chem* 86:10796–10803
- Keller M, Naue J, Zengerle R, von Stetten F, Schmidt U (2015) Automated forensic animal family identification by nested PCR and melt curve analysis on an off-the-shelf thermocycler augmented with a centrifugal microfluidic disk segment. *PLoS ONE* 10:e0131845
- Laser ablation (2018) Wikipedia
- Ma H, Horiuchi KY, Wang Y, Kucharewicz SA, Diamond SL (2005) Nanoliter homogenous ultra-high throughput screening microarray for lead discoveries and IC50 profiling. *Assay Drug Dev Technol* 3:177–187
- Mao S, Zhang J, Li H, Lin J-M (2013) Strategy for signaling molecule detection by using an integrated microfluidic device coupled with mass spectrometry to study cell-to-cell communication. *Anal Chem* 85:868–876
- Neu V, Steiner R, Müller S, Fattinger C, Zenobi R (2013) Development and characterization of a capillary gap sampler as new microfluidic device for fast and direct analysis of low sample amounts by ESI-MS. *Anal Chem* 85:4628–4635
- Neu V, Dörig P, Fattinger C, Müller S, Zenobi R (2016) Characterization of a miniaturized liquid bridge for nL sample infusion: a comparative study of sample flush-out behavior using flow simulations and direct ESI-MS analysis. *Microfluid Nanofluidics* 20:62

- Ozbal CC et al (2004) High throughput screening via mass spectrometry: a case study using acetylcholinesterase. *Assay Drug Dev Technol* 2:373–381
- Rodenstein M, Zürcher S, Tosatti SGP, Spencer ND (2010) Fabricating chemical gradients on oxide surfaces by means of fluorinated, catechol-based, self-assembled monolayers. *Langmuir* 26:16211–16220
- Sreekumar A et al (2009) Metabolomic profiles delineate potential role for sarcosine in prostate cancer progression. *Nature* 457:910–914
- Stark T, Wollmann N, Lösch S, Hofmann T (2011) Quantitation of resveratrol in red wines by means of stable isotope dilution analysis—ultra-performance liquid chromatography—quantime-of-flight mass spectrometry and cross validation. *Anal Chem* 83:3398–3405
- Strohmeier O et al (2015) Automated nucleic acid extraction from whole blood, *B. subtilis*, *E. coli*, and Rift Valley fever virus on a centrifugal microfluidic LabDisk. *RSC Adv* 5:32144–32150
- Sun S, Kennedy RT (2014) Droplet electrospray ionization mass spectrometry for high throughput screening for enzyme inhibitors. *Anal Chem* 86:9309–9314
- van Reenen A, de Jong AM, den Toonder JMJ, Prins MWJ (2014) Integrated lab-on-chip biosensing systems based on magnetic particle actuation—a comprehensive review. *Lab Chip* 14:1966–1986
- Wan H et al (2003) High-throughput screening of pKa values of pharmaceuticals by pressure-assisted capillary electrophoresis and mass spectrometry. *Rapid Commun Mass Spectrom* 17:2639–2648
- Wohlfarth C (2008) Surface tension of pure liquids and binary liquid mixtures: (supplement to IV/16). Springer, Berlin
- Zhang S, Pelt CKV (2004) Chip-based nanoelectrospray mass spectrometry for protein characterization. *Expert Rev. Proteomics* 1:449–468

**Publisher's Note** Springer Nature remains neutral with regard to jurisdictional claims in published maps and institutional affiliations.